Indian Journal of Pure & Applied Physics
Vol. 59, July 2021, pp. 513-521

Computational, Spectral & Single Crystal Studies of 4-chloro-N,Ndiphenylbenzamide

Shraddha Shukla[a], Abha Bishnoi[a*], Poornima Devi[a], Shaheen Fatma[b] & Ramesh Singh[c]

[a]Department of Chemistry, Lucknow University, Lucknow 226 007, India
[b]Department of Chemistry, Shri Ram swaroop Memorial University, Lucknow Dewa Road, Barabanki 225 003, India
[c]Indian Institute of Technology, Kalyanpur, Kanpur, Uttar Pradesh 208 016, India

Received 1 August 2019; accepted 8 June 2021

The present work comprises of spectroscopic, crystal and *in silico* studies of 4-chloro-N,Ndiphenylbenzamide. Synthesis of the compound was done followed by respective characterization by different spectral approaches. The *in silico* studies of title compound was further performed to ascertain various structural and geometrical parameters. All the studies were carried out at thetheory level B3LYP functional and 6-31G (d, p) as basis set. The geometry and other structural aspects of 4-chloro-N,Ndiphenylbenzamide were confirmed by X-ray diffraction.

Keywords: Spectroscopic, Structural, Parameters

1 Introduction

It is reported in the literature that amide compounds exhibit a wide range of bioactive properties[1-4]. The amide dervatives have special significance as this functional group is present in the structure of many natural products and drugs. Some amide derivatives are reported to possess plant fungicidal activity such as carboxamide fungicides eg. benodanil, mepronil and flutolanil. The biological activities of these derivatives are due to the presence of benzamide nucleus that can be lethal to the growth of pathogenic fungi[5,6]. Benzamide moiety has also been studied as possible metabolite of many antibacterial compounds like oxazolidinone, oxyclozanide[7,8].

X ray crystallography along with computational method, accounts for unusual electronic properties of a material and throws light on chemical interactions which aids in designing pharmaceuticals against many diseases. Considering all these aspects, 4-chloro-N,Ndiphenylbenzamide became the subject of interest for the authorsas the literature survey revealed that *in silico* studies and X ray crystallography for the compound 3 has not been previously performed. In the present study, various theoretical aspects such as NLO, NBO, MESP and thermodynamic properties were investigated by computational method along with spectral characterization of title compound. In addition to it, single crystal X-ray diffraction was employed for précised determination of various cell parameters of compound 3, including cell dimensions and positions of atoms within the lattice. The results thus obtained from crystal studies were correlated with computational and experimental data.

2 Computational details

The *in silico* studies were performed with the help of DFT using Gaussian 09 program package[9] without involving any geometrical constraint[10]. The NBO calculations[11] were carried out at DFT/B3LYP level to predict various second order interactions.

3 Results and discussion

3.1 Materials and method

The spectrophotometers used for spectral analysis of molecule are-Bruker 400 MHz for NMR, Perkin-Elmer Fourier transform for IR and Double-Beam spectrophotometer for UV spectroscopy. The solvent used was $CDCl_3$ while tetramethylsilane served the purpose of internal reference.

3.1.1 General method of preparation of 4-chloro-N, N diphenylbenzamide

The schematic route for preparation of 4-chloro-N, Ndiphenylbenzamide (3) has been illustrated in Scheme 1. 4-chloro-N, N diphenylbenzamide (3) was prepared according to the previously reported procedure[12]. Diphenylamine (0.01 mol) (1) and pyridine (0.01 mol) were dissolved in 12.5 ml CH_2Cl_2.

*Corresponding author (E-mail: abhabishnoi5@gmail.com)

The reaction mixture was constantly stirred with slow addition of 4 chlorobenzoyl chloride (0.02 mol) (2) till the product (3) was obtained with ~70% yield as per scheme 1. The crude product was recrystallized from ethanol affording colourless needle shaped crystals.

3.2 Molecular geometry

The optimised structural parameters for 3 are tabulated in Table S1 whereas Fig. 1 contains the optimised structure. Marked changes in several features such as electronic and spectroscopic are possible due to a small change in the geometry of the molecules. Thus it was essential to examine the optimized geometry of the studied molecule (3).The longest bond length was found between C19-Cl22 with the calculated value of 1.757 Å, same as the experimental value (1.741Å). The minimum bond length was observed in C13-H31 with the value of 1.083 Å as computed one and 0.95 Å as determined from X-ray crystallography respectively. All carbon-carbon and carbon-hydrogen bond distances of rings were found to be in the range of 1.393-1.505 Å and 1.083-1.085 Å respectively. Presence of lone pair, electronegativity and the conjugation present in the molecule contributed to the variations observed in the various bond angles in the molecule.

3.3 X-ray studies

X-ray diffraction data was recorded on a Bruker APEX-II Quasar CCD area-detector diffractometer. Bruker software package SAINT[13] and SADABS[14] were used for data reduction and absorption corrections. SHELXS-97[15] was used to solve the structure and was refined by employing SHELXL-97[16] package. Crystallographic results are presented in

Table 1,S2(a), S2(b) and S2(c). Recrystallization of 3 was carried out in ethanol resulting in pure crystals. ORTEP diagram of 3 and its molecular packing are shown in Figs. 2(a-b) respectively. As evident from

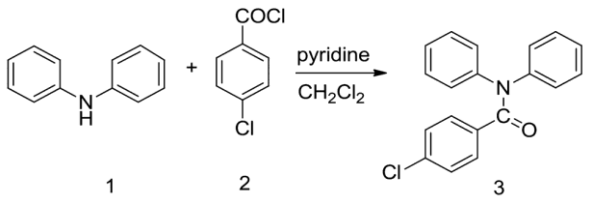

Scheme 1 — Synthesis of compound **3**.

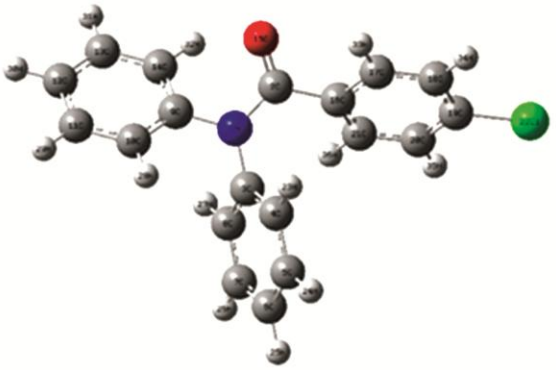

Fig. 1 — Optimized Structure of compound 3.

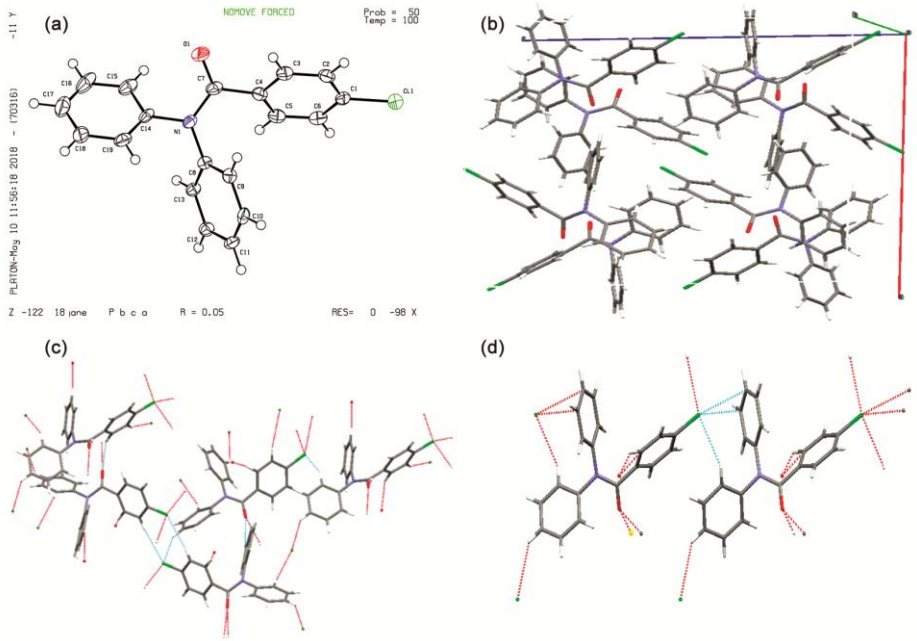

Fig. 2 — (a) ORETP diagram of compound 3 drawn at 50% probability level, (b) Molecular packing in the crystal structure, (c) Hydrogen bonding interactions (dashed lines) in the crystal structure and (d) Short intermolecular interactions (dashed lines) in the crystal structure.

crystallographic data, the compound contains three aromatic rings with all the bond distances lying in appropriate ranges. The C-N distances (N1-C7=1.371 (3) Å, N1-C8=1.438(3) Å, N1-C14=1.437(3) Å) are in normal range and in good compliance with previously reported literatures. The bond angles around nitrogen atom (C14-NI-C8=117.62(19) Å, C8-N1-C7=123.40(2) Å, C14-N1-C7=118.32(19) Å) correspond to a value of 359.34 (4) Å thus suggesting sp^3 hybridisation[17].The carbon-hydrogen distances were observed at 0.95 Å. The presence of C=O group contracts the bond angles (C7-N1-C14=118.32(19) Å and C14-N1-C8=117.62(19) Å), while it expands the bond angle C7-N1-C8 with a value of 123.4(2) Å. The two phenyl rings of the amine moiety are neither fused to each other nor to the chlorophenyl ring. The two phenyl rings C14/C19/C15/C18/ C16/C17 and C13/C12/C8/C11/C10/C9 are almost perpendicular to one another separated by a distance of 4.801 Å. The centroid distance between chlorophenyl ring C6/C3/C1/C2/C5/C4 and phenyl ring C14/C19/C15/C18/C16/C17 is 6.499 Å while the centroid distance between the other phenyl ring C13/C12/C8/C11/C10/C9 and the chloro phenyl ring is 4.452 Å.

The molecule is stabilized by intermolecular hydrogen bonging and six short intermolecular interactions, results of which are tabulated in **S2(d)**. The H-bonding interactions are shown in Figs. 2(c-d) respectively. The intermolecular hydrogen bond distances range from 2.876 Å for Cl1-H15 , 2.813 Å for O15-H26, 2.872 Å for Cl1-H17, 2.955 Å for Cl1-H6 and 2.348 Å for Cl1-H5 respectively. The other six interactions are seen between Cl1-H19 (2.876 Å), Cl1-C12 (3.448 Å), Cl1-C11 (3.417 Å), Cl1-H17 (2.872 Å), O1-H5 (2.348 Å) and O1-C5 (3.183 Å).

3.4 NMR and vibrational assignments

For NMR computations (^1H &^{13}C), GIAO approach was incorporated using B3LYP method[18]. The corresponding NMR data has been tabulated in Table 2(a). The correlation graphics between the

Table 1 — Data collection and structure refinement for crystal.

Chemical formula	$C_{19}H_{14}ClNO$	
Formula weight	307.76 g/mol	
Temperature	100(2) K	
Wavelength	0.71073 Å	
Crystal size	0.120 x 0.190 x 0.230 mm	
Crystal system	orthorhombic	
Space group	P b c a	
Unit cell dimensions	a = 17.5881(5) Å	α = 90°
	b = 8.8499(2) Å	β = 90°
	c = 19.7370(6) Å	γ = 90°
Volume	3072.12(15) $Å^3$	
Z	8	
Density (calculated)	1.331 g/cm^3	
Absorption coefficient	0.249 mm^{-1}	
F(000)	1280	
Theta range for data collection	2.78 to 25.05°	
Index ranges	-20<=h<=20, -10<=k<=10, -23<=l<=23	
Reflections collected	35002	
Independent reflections	2726 [R(int) = 0.0289]	
Coverage of independent reflections	99.8%	
Absorption correction	Multi-Scan	
Max. and min. transmission	0.9710 and 0.9450	
Structure solution technique	direct methods	
Structure solution program	XT, VERSION 2014/5	
Refinement method	Full-matrix least-squares on F^2	
Refinement program	SHELXL-2014/7 (Sheldrick, 2014)	
Function minimized	$\Sigma w(F_o^2 - F_c^2)^2$	
Data / restraints / parameters	2726 / 0 / 199	
Goodness-of-fit on F^2	1.614	
Final R indices	2510 data; I>2σ(I)	R1 = 0.0533, wR2 = 0.1965
	all data	R1 = 0.0567, wR2 = 0.2006
Weighting scheme	$w=1/[\sigma^2(F_o^2)+(0.1000P)^2+0.5396P]$ where $P=(F_o^2+2F_c^2)/3$	
Largest diff. peak and hole	1.227 and -0.594 $eÅ^{-3}$	
R.M.S. deviation from mean	0.062 $eÅ^{-3}$	
CCDC No.	1896093	

calculated and experimental values, following the linear equations, $y = 0.3836x + 2.1735$ for ^{1}H NMR and $y = 1.0926x - 11.137$ for ^{13}C NMR, has been depicted in Fig. 3. Computational data revealed that all aromatic hydrogens appeared in the range of δ6.97-8.09 which showed agreement with the experimental values ranging from δ7.126-7.408. The multiplet of four deshielded protons appeared at positions C4, C8, C10, C14 at δ 7.22-7.18, a multiplet

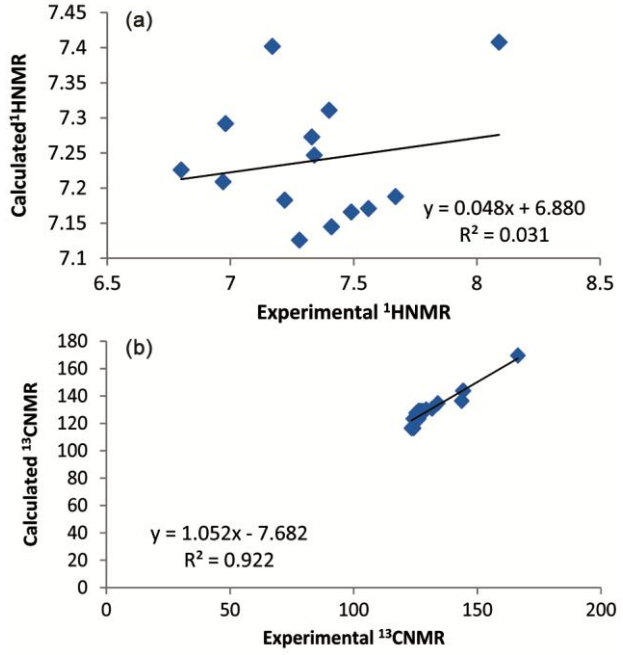

Fig. 3 — Correlation graph (a) between experimental and calculated ^{1}HNMR chemical shifts and (b) between experimental and calculated ^{13}C NMR chemical shifts using B3LYP/6-31G (d, p).

at δ 7.17-7.12 for four protons appeared at C5, C8, C11 and C13 and two triplets at δ 7.40-7.39 and δ7.38-7.37 for one proton each appeared at C6 and C12. The hydrogen attached to carbon adjacent to carbonyl group showed computational and experimental shift as δ7.4 and 7.27-7.24 respectively depicting good agreement between the two values. The hydrogen attached to the carbon adjacent to chlorine group appeared at δ 7.17 and 7.31-7.29 respectively as computed theoretically and experimentally. Two molecular ions with m/z ; 307.08 and 309.07 with a base peak of m/z 146 (M – C_6H_4Cl), were obtained affirming the proposed structure for **3.**

The signals at δ 143.81 and 136.44 are due to carbons attached to nitrogen and chlorine atom respectively. The signal at δ 126.74 ppm corresponded to the carbon adjacent to -C=O group. The ring carbons of amine moiety appeared at δ 127.58, 129.40 and 126.74. The carbon signals observed at δ 128.34 and 130.81 are due to phenyl ring carbons near to chlorine and carbonyl group respectively.

The calculated ^{13}C shifts for C2 at δ 166.39 matched well with experimental shift at 169.64 confirming carbonyl carbon in an amide linkage. The experimental ^{1}H and ^{13}C NMR are given in Fig. S1 and S2.

The experimental and calculated vibrational wavenumbers are given in Table 2(b). Computed wave numbers scaled down by a factor 0.9679 for B3LYP[19]. Fig. 4 contains the correlation graphics depicting a correlation coefficient value of 0.994

Table 2 (a) — Experimental and calculated ^{1}H NMR and ^{13}C NMR chemical shifts of title compound using DFT/B3LYP 6-31G (d,p).

Atom no.	Calculated	Experimental	Atom no.	Calculated	Experimental
2C	166.39	169.64	23H	6.97	7.209
3C	144.12	143.81	24H	7.28	7.126
4C	128.32	128.34	25H	7.33	7.273
5C	126.97	129.14	26H	7.49	7.166
6C	124.2	116.51	27H	7.22	7.183
7C	127.83	129.14	28H	6.8	7.226
8C	125.37	123.35	29H	7.41	7.145
9C	144.39	143.81	30H	7.34	7.247
10C	124.09	123.35	31H	7.56	7.171
11C	126.94	129.14	32H	7.67	7.188
12C	123.36	116.51	33H	8.09	7.408
13C	126.24	129.14	34H	7.4	7.311
14C	126.32	123.35	35H	6.98	7.292
16C	134.01	134.66	36H	7.17	7.402
17C	131.66	130.81			
18C	126.99	126.74			
19C	143.66	136.44			
20C	125.22	127.58			
21C	129.33	130.19			

between experimental and calculated wave numbers where as the theoretical and recorded IR spectra are shown in Fig. S3 and Fig. 5 respectively**.**

An intense band at 1690.92 cm^{-1} appeared due to the -C=O stretching motion[20] which was in compliance with the experimental band at 1651.01 cm^{-1}. The aromatic -C–H stretching vibrations[21] appeared at 3081.03 cm^{-1} with experimental value at 3100 cm^{-1}. The ring carbon-carbon stretching vibrations for **3** appeared at 1591.80 cm^{-1} with the experimental value at 1589.34 cm^{-1}.The calculated and experimental -C-N stretching vibration[22] was observed at 1259.23 and 1344.38 cm^{-1} respectively. Anote worthy correlation between theoretical and recorded C–Cl stretching[23] was further evident (669.90 cm^{-1} and 692.44 cm^{-1}).

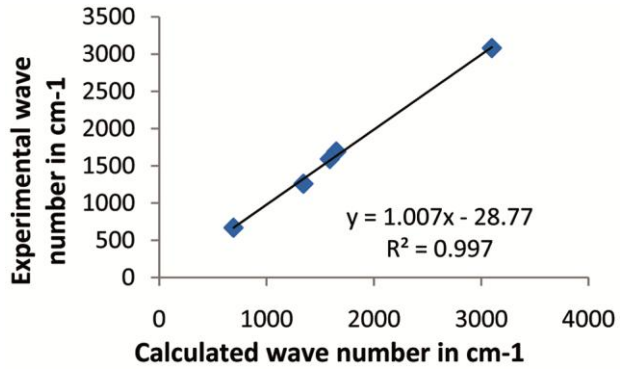

Fig. 4 — Correlation graph between experimental and calculated wavenumbers using B3LYP/6-31G.

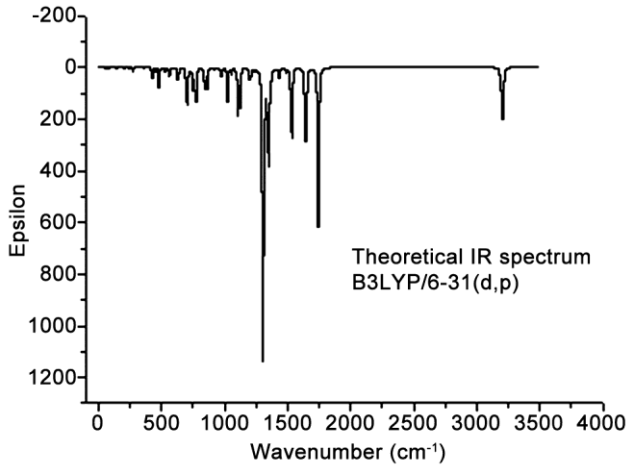

Fig. 5 — Theoretical IR spectra of Compound 3

Table 2(b) — Experimental and calculated FT-IR vibrations of title compound using DFT/B3LYP 6-31G (d,p).

Experimental	Calculated B3LYP	Vibrational Assignment
1651.01	1690.92	C=O stretching
3100	3081.03	=CH stretching
1589.34	1591.8	C=C stretching
1344.38	1259.23	C-N stretching
692.44	669.9	C-Cl stretching

3.5 UV-Visible spectral studies

UV-Vis spectral studies showed electronic transitions at 309 nm from HOMO→LUMO (*f*=0.1686, π →π*) with percentage contribution of 20% and a transition at 234 nm from HOMO-4→LUMO (*f*=0.1706, n→π*) which agreed well with the observed values at 310 and 275 nm respectively. The values obtained for the energy gap suggest the relative steadiness of the compound **3**. Table 3 contains the corresponding UV data. The compared experimental data and the calculated values is shown in Fig. 6 whereas Fig. 7 shows the HOMO-LUMO mapping.

3.6 Molecular electrostatic potential

It is a well known fact that the action centres for robust nucleophilic activity as well as electrophilic

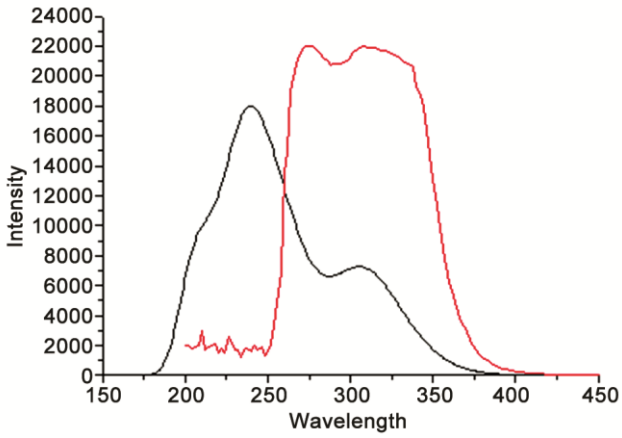

Fig. 6 — Theoretical and Experimental UV-visible spectrum of compound 3.

Table 3 — Experimental and theoretical absorption wavelength λ (nm), excitation energies E (eV) of title compound using B3LYP functional and 6-31-G/ (d, p) basis set.

Compound	Major contributing Molecular orbitals	E (eV)	Calculated (λ_{max})	Assignment	Oscillatory strength
	H→L (20%)	4.012	309	π →π*	0.1686
	H-4→L (44%)	5.287	234	n→π*	0.1706

actvity[24] can be studied effectively by employing molecular electrostatic potential (MESP) approach. MESP sketch representing the relative reaction tendencies of atoms[25] is shown in Fig. 8. While the red region (C2 and O15) depicted the site of electrophilic activity (MESP value = -5.81 a.u.) , a possible attack by nucleophile can be very well predicted by blue regions (C5, C6 and C7) of the map (MESP value = +5.81 a.u.).

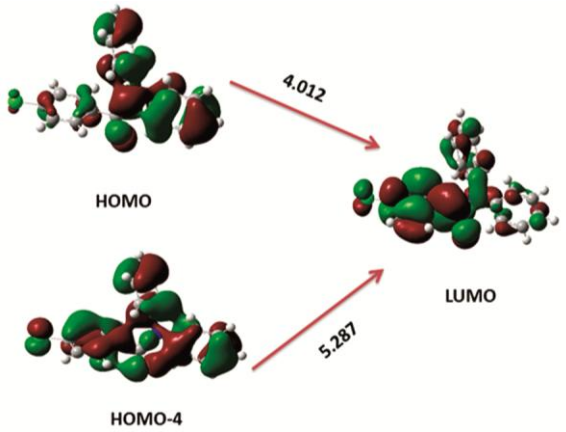

Fig. 7 — HOMO-LUMO energy gap diagram involved in electronic transitions in isolated (gaseous) phase of compound 3.

3.7 Natural bond orbital analysis

NBO[26] is a conducive approach for the exploration of transfer of charge within the molecule. As the interaction between electron donors and acceptors advances, the value of stabilization energy also enhances. Interactions between contributor bonds and receiver bonds were analyzed with the help of second order Fockmatrix[27].

Table 4 contains the relevant NBO data. As per the analysis, significant transfer of charge in the compound 3 was observed from π (C_{19}-C_{20}) to π* (C_{16}-C_{21}),π (C_{19}-C_{20}) to π* (C_{17}-C_{18}) and n→π * from N_1 to C_2-O_{15} with stabilization energy of 201.04, 143.14 and 38.52 kcal mol^{-1} respectively depicting relocation of electrons from the heteroatom to π system. Other than these transistions, several π→π * and n→π* intramolecular transistions were also seen with stabilisation energy values ranging between 20-30 kcal mol^{-1}.

3.8 Non -linear optical analysis

The computational approach is very utilitarian for analysing the NLO properties of molecules. The non-linear optical properties have applications indifferent

Table 4 — Second order perturbation theory analysis of Fock matrix in NBO basis of compound 3.

Donor (i)	Type	Ed/e	Acceptor (i)	Type	Ed/e	E(2)a	E(j)a E(i)b	F(I,j)c
BD(2) C3-C4	π	1.664	BD*(2) C5-C6	π*	0.3283	19.91	0.29	0.07
BD(2) C3-C4	π	1.664	BD*(2) C7-C8	π*	0.3215	19.02	0.29	0.07
BD(2) C5-C6	π	1.662	BD*(2) C3-C4	π*	0.3766	20.6	0.27	0.07
BD(2) C5-C6	π	1.662	BD*(2) C7-C8	π*	0.3766	20.78	0.28	0.07
BD(2) C7-C8	π	1.675	BD*(2) C3-C4	π*	0.3215	20.6	0.28	0.07
BD(2) C7-C8	π	1.675	BD*(2) C5-C6	π*	0.3283	19.38	0.28	0.07
BD(2) C9-C10	π	1.664	BD*(2) C11-C12	π*	0.3348	20.14	0.29	0.07
BD(2) C9-C10	π	1.664	BD*(2) C13-C14	π*	0.3177	19.15	0.29	0.07
BD(2) C11-C12	π	1.666	BD*(2) C9-C10	π*	0.3711	20.45	0.28	0.07
BD(2)C11-C12	π	1.666	BD*(2) C13-C14	π*	0.3177	20.18	0.28	0.07
BD(2)C13-C14	π	1.669	BD*(2) C9-C10	π*	0.3177	20.77	0.28	0.07
BD(2)C13-C14	π	1.669	BD*(2) C11-C12	π*	0.3344	20.05	0.28	0.07
BD(2)C16-C21	π	1.641	BD*(2) C17-C18	π*	0.3	15.06	0.3	0.06
BD(2)C16-C21	π	1.641	BD*(2) C17-C18	π*	0.3	20.75	0.28	0.07
BD(2)C16-C21	π	1.641	BD*(2) C19-C20	π*	0.3888	20.99	0.27	0.07
BD(2)C17-C18	π	1.658	BD*(2) C16-C21	π*	0.3653	18.68	0.28	0.07
BD(2)C17-C18	π	1.658	BD*(2) C19-C20	π*	0.3888	22.05	0.27	0.07
BD(2)C19-C20	π	1.67	BD*(2) C16-C21	π*	0.3653	19.67	0.3	0.07
BD(2)C19-C20	π	1.67	BD*(2) C17-C18	π*	0.3	17.83	0.3	0.07
LP(1) N1	n	1.683	BD*(2) C2-O15	π*	0.2666	38.52	0.3	0.1
LP(1) N1	n	1.683	BD*(2) C3-C4	π*	0.3766	12.25	0.28	0.05
LP(1) N1	n	1.683	BD*(2) C9-C10	π*	0.3711	13.52	0.29	0.06
LP(2) O15	n	1.861	BD*(1) N1-C2	σ*	0.0905	27.81	0.67	0.12
LP(2) O15	n	1.861	BD*(1) C2-C16	σ*	0.0658	19.28	0.66	0.1
LP(3) Cl22	n	1.928	BD*(2) C19-C20	π*	0.3888	12.29	0.33	0.06
BD*(2)C2-O15	π	0.262	BD*(1) C2-O15	π*	0.2616	5.87	0.52	0.13
BD*(2) C6-C21	π	0.365	BD*(2) C2-O15	π*	0.2616	94.88	0.02	0.07
BD*(2) C19-C20	π	0.389	BD*(2) C16-C21	π*	0.3653	201	0.02	0.08
BD*(2) C19-C20	π	0.389	BD*(2) C17-C18	π*	0.3	143.4	0.02	0.08

Table 5 — Calculated ε_{LUMO}, ε_{HOMO}, energy band gap ε_{LUMO}– $\varepsilon_{HOMO,}$ ionization potential (IP), electron affinity (EA), electronegativity (χ), global hardness (η), chemical potential (μ), global electrophilicity index (ω), global softness (S) and additional electronic charge (ΔN max) in eV for assayed compound, using DFT/B3LYP/6-31G(d, p).

ϵ_H	ϵ_L	ϵ_H-ϵ_L	I	A	χ	η	μ	ω	S
-2.1794	-0.0484	-2.1309	2.1794	0.0484	1.1139	1.0653	-1.1139	0.5823	0.4693

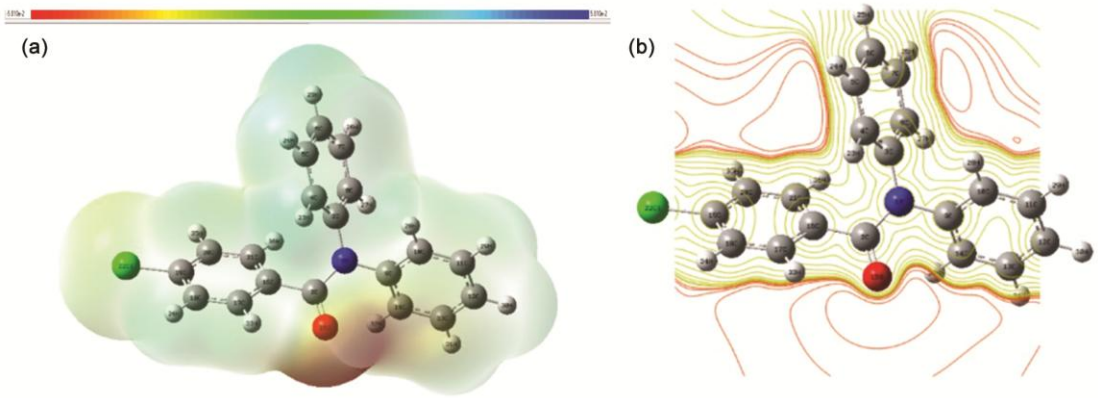

Fig. 8 — 3D and 2D plots of the molecular electrostatic potential of title compound 3.

areas as telecommunications, optical interconnections *etc*.[28-30]. An aromatic organic system substituted with electron donating and electron accepting groups, give rise to a high nonlinear optical coefficient, thus increasing the polarisation. The overall calculations for NLO parameters were done as per Kleinman symmetry[31].

The corresponding data of μ_i (i = x, y, z), α_{ij} and βijk are presented in Table S2. The calculated dipole moment and polarizability for **3** are found to be 3.41 D, and 0.00014238×10^{-24}esu respectively. Also the value of first hyperpolarizability for the molecule under consideration (**3**) is found to be 0.00944×10^{-30} esu respectively comparable to that of urea ($\beta_{tot}= 0.378\times10^{-30}$esu), having non linear properties[32], further suggesting the molecule to be a potent NLO material. The presence of π conjugated system within the molecule confirms it non-linearity.

3.9 Thermodynamic properties

The thermodynamic data provides many useful informations in consistence with the interactions of thermodynamic functions as per 2nd law of thermodynamics[33]. All thermodynamic parameters of compound under consideration are reported in Table S3 and S4. All calculated values are tabulated in Table S5. Results indicated that the corresponding enhancement in standard thermodynamical parameters with increasing temperature can be attributed to the progression in intensities of vibrations with increasing temperature[34, 35]. Figure 9 contains the correlation graphics.

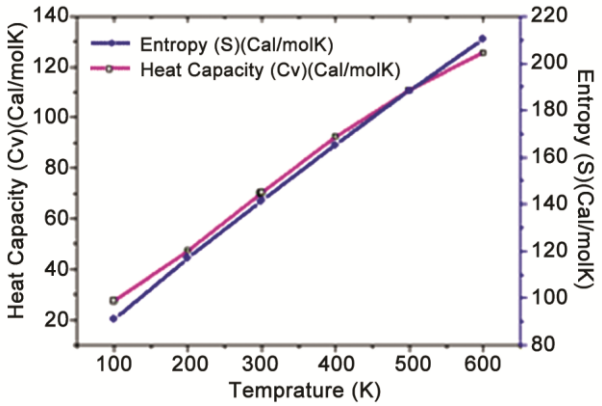

Fig. 9 — Graphical representation of correlation of heat capacity and entropy calculated at different temperatures using B3LYP/6-31G (d, p).

3.10 Reactivity descriptors

3.10.1 Global reactivity descriptors

The global reactivity descriptors[36-40] are used extensively to elucidate mechanistic pathway and sites of chemical reactivity in molecules. Energies of frontier molecular orbital (ε_{LUMO}, ε_{HOMO}), band gap (ε_{LUMO}- ε_{HOMO}) and other such descriptors are reported in Table 5. As the chemical potential (-1.1139) for compound **3** comes out to be negative, hence the stability of the compound can be easily predicted.

3.10.2. Local reactivity descriptors

The maximum values of local reactivity descriptors indicate the sites that are more prone to the attack of a nucleophile and electrophile. The various reactivity

Table 6 — Fukui functions (fk^+, fk^-), Local softnesses (sk^+,sk^-) in eV, local electrophilicity indices (ωk+, ωk-) in eV for specific atomic sites of compound 3.

Atoms	q_N	q_N+1	q_N-1	f_k+	f_k-	sk^+	sk^-	ωk+	ωk-
1 N	-0.61162	-0.5517	0.263596	0.059917	-0.87521	0.015445	-0.22554	0.219338	-3.20388
2 C	0.510518	0.518227	-0.04424	0.007709	0.554758	0.001987	0.142961	0.02822	2.030803
3 C	0.207773	0.199661	0.039662	-0.00811	0.168111	-0.00209	0.043322	-0.0297	0.615404
4 C	0.018584	0.074384	0.069187	0.0558	-0.0506	0.014384	-0.01304	0.204267	-0.18524
5 C	-0.00112	0.055435	-0.03615	0.056556	0.035027	0.014579	0.009026	0.207035	0.128223
6 C	0.012296	0.098766	0.139063	0.08647	-0.12677	0.02229	-0.03267	0.316541	-0.46406
7 C	-0.00142	0.055498	-0.04427	0.056918	0.042846	0.014672	0.011041	0.20836	0.156846
8 C	0.014439	0.064022	0.077945	0.049583	-0.06351	0.012782	-0.01637	0.181508	-0.23248
9 C	0.261355	0.262168	0.078739	0.000813	0.182616	0.00021	0.04706	0.002976	0.668502
10 C	0.00672	0.068544	0.079973	0.061824	-0.07325	0.015937	-0.01888	0.226319	-0.26816
11 C	-0.01013	0.053975	-0.04172	0.064109	0.031586	0.016526	0.00814	0.234684	0.115627
12 C	0.008158	0.107999	0.174982	0.099841	-0.16682	0.025737	-0.04299	0.365488	-0.61069
13 C	-0.01113	0.054243	-0.0445	0.065376	0.033365	0.016853	0.008598	0.239322	0.122139
14 C	0.032011	0.095449	0.077158	0.063438	-0.04515	0.016353	-0.01163	0.232227	-0.16527
15 O	-0.48706	-0.42778	0.062013	0.059282	-0.54908	0.015282	-0.1415	0.217014	-2.01
16 C	0.029557	0.028653	0.062095	-0.0009	-0.03254	-0.00023	-0.00839	-0.00331	-0.11911
17 C	0.032794	0.066992	-0.00485	0.034198	0.037648	0.008816	0.009702	0.125189	0.137818
18 C	0.035508	0.085102	0.014748	0.049594	0.02076	0.012784	0.00535	0.181549	0.075996
19 C	-0.08895	-0.08522	0.045127	0.003728	-0.13408	0.000961	-0.03455	0.013647	-0.49081
20 C	0.034413	0.073994	-0.00895	0.039581	0.043361	0.010203	0.011174	0.144894	0.158732
21 C	0.023902	0.030814	0.012986	0.006912	0.010916	0.001782	0.002813	0.025303	0.03996
22 Cl	-0.0166	0.07077	0.027401	0.087365	-0.044	0.022521	-0.01134	0.319817	-0.16106

descriptors, softnesses and electrophilicity indices[40] of studied moiety are reported in Table 6.

The significant increase in the values of f_k^+, s_k^+, ω_k^+, evident at C6, C12 and Cl22 indicated that these reaction centres are more prone to nucleophilic attack, while the elevated values of f_k^-, s_k^-, ω_k^- at C2, C3 and C9 suggested that these sites could be a target for electron deficient species.

4 Conclusion

The present work involves detailed structural elucidation and subsequent characterization of **4-chloro-N, N diphenylbenzamide** by crystallographic, computational and spectral techniques, which affirmed the structure of the molecule. DFT studies revealed that all the computed and experimental values are in good relation with each other. The structural and symmetry properties of compound **3** were explored by electrostatic potential surfaces (ESP). Crystal studies affirmed the orthorhombic structure of **3** with most of the optimised parameters complying with computed values. Chemical reactivity of the compound was ascertained by reactivity descriptors. The values of partial dipole momentand polarizability suggested that the molecule can be a NLO material. A corresponding enhancement is seen in thermodynamic parameters as the temperature was increased. Also, natural bond orbital (NBO) analysis depicted the movement of electrons within **3**.

Supporting information

The tables containing crystallographic data, optimized parameters, NLO studies, thermodynamic data as well as spectral data of compound **3** are provided as supporting information.

Acknowledgement

The authors express their sincere gratitude to the Head, Department of Chemistry, Lucknow University, Lucknow, for providing laboratory facilities. Authors are also thankful to the Director, CDRI, Lucknow for spectral analysis and to the Director, IIT Kanpur for providing crystallographic data.

Conflict of interest

The authors report no conflict of interest**.**

References

1 Desai P S & Desai R, *J Ind Chem Soc*, 70 (1993) 177.
2 Paul P C, Bedi P K &Vashisht K K,*J Ind Chem Soc*,53 (1976) 768.
3 Shah V H, Patel H H & Parikh A R, *J Indian Chem Soc*, 59 (1982) 678.
4 Hamurcu F, Gunduzalp A B, Cete S & Erk B,*Transist Metal Chem*, 33 (2003) 137.
5 Huang Q C,*Worldpestic*, 26 (2004) 23.

6 Leroux P, *Pestic Sci*, 47 (1996) 191.
7 Cui Y, Dang Y, Yang Y & Ji R,*Curr Sci*, 89 (2005) 531.
8 HishanoT, Ichikawa M, TsumotoK & Tasaki M, *Chem Pharm Bull*, 30 (1982) 2996.
9 Frisch M J, Trucks G W, Schlegel H B, Scuseria G E, Robb M A, Cheeseman J R, Scalmani G, Barone V, Mennucci B, Petersson G A, Nakatsuji H, Caricato M, Li X, Hratchian H P, Izmaylov A F, Bloino J, Zheng G, Sonnenberg J L, Hada M, Toyota K R, Fakuda J, Hasegawa, Ishida M, Nakajima T, Honda y, Kitao O, Nakai H, Vreven T, Montgomery J A Jr Peralta J E, Ogliaro F, Bearpark M, Heyd J J, Brothers E, Kudin K N, Staroverov V N, Kobyashi R, Normand J, Raghavachari K, Rendell A, Burant J C, Iyengar S S, Tomasi J, Cossi M, Rega N, Millam J M, Klene M, Knox J E, Cross J B, Bakken V, Adamo C J, Cammi R, Pomelli C, Ochterski JW, Martin R L, Morokuma K, Zakrzewski V G, Voth G A, Salvador P, Dannenberg J J, Dapprich S,Daniels A D, Farkas O, Foresman J B, Ortis J V, Ciolowaski J & Fox D J, Gaussian-09, Revision A.02, *Gaussian Inc*, (Wallingford CT), 2009.
10 Schlegel H B, *J Comput Chem*, 3 (1982) 214.
11 Chaitanya K, Santhamma C, Prasad K, Prasad V & Veeraiah V, *J Atom Mol Sci*, 3 (2012) 1.
12 Tang X, Chen S & Wang L, *Asian J Chem*, 24 (2012) 24.
13 SAINT+, version 6.02; Bruker AXS: *Madison*, WI, 1999.
14 Sheldrick G M, SADABS, *Empirical Absorption Correction Program*, University of Gottingen: Gottingen, Germany, 1997.
15 Sheldrick G M, SHELXTL Reference Manual, version 5.1, Bruker AXS, *Madison*, WI, 1997.
16 Sheldrick G M, SHELXL-97, *Program for Crystal Structure Refinement*, University of Gottingen, Gottingen, Germany, 1997.
17 Beddoes R L, Dalton L, Joule T A, Mills O S, Street J D & Watt C I F, *J Chem Soc Perkin Trans*, 2 (1986) 787.
18 Schuchardt K L, Didier B T, Elsethagen T, Sun L, Gurumoorthi V, Chase J, Li J & Windus T L, *J Chem Inf*, (2007) 1045.
19 Hiroshi Y & Akito E,*Chem Phys Lett*, 325 (2000) 477.
20 Karabacak M, *J Mol Struct*, 919 (2009) 215.
21 Varsanyi G, *Vibrational Spectra of Benzene Derivatives*, Academic Press, New York, 1969.
22 Krishnakumar V, Manohar S & Nagalakshmi R, *J Spectrochim Acta*, 71 (2008) 110.
23 Mooney E F,*J Spectrochim Acta*, 19 (1963) 877.
24 Politzer P & Murray J S, *Theoretical biochemistry and molecular biophysics: a comprehensive survey*,in: Beveridge D L & Lavery R, Eds, 1991.
25 Gupta V P, Sharma A, Virdi V & Ram V J, *J Spectrochim Acta*, 64 (2006) 57.
26 Glendening E D, Reed A E, Carpenter J E & Weinhold F, NBO Version 3.1, TCI, University of Wisconsin, *Madison*, 1998.
27 Reed A E, Curtis L A & Weinhold F,*Chem Rev*, 88 (1988) 899.
28 Andraud C, Brotin T, Garcia C, Pelle F, Goldener P, Bigot B & Collet A, *J Am Chem Soc*, 116 (1994) 2094.
29 Nakano M, Fujita H, Takahata M & Yamaguchi K, *J Am Chem Soc*, 124 (2002) 9648.
30 GeskinV M, Lambert C & Bredas J L, *J Am Chem Soc*, 125 (2003) 15651.
31 Kleinman D A, *Phys Rev*, 126 (1962) 1977.
32 Madhurambal G & Mariappan M, *Indian J Pure Appl Phys*, 48 (2010) 264.
33 Zhang R, Dub B, Sun G & Sun Y, *J Spectrochim Acta*, 75 (2010) 1115.
34 Ott J B & Goates J B, *Calculations from statistical Thermodynamics*, Academic Press, 2000.
35 Sajan D, Josepha L, Vijayan N & Karabacak M, *J Spectrochim Acta*, 81 (2011) 85.
36 Pearson R G, *J Org Chem*, 54 (1989) 1430.
37 Parr R G & Pearson R G, *J Am Chem Soc*, 105 (1983) 7512.
38 Geerlings P, Proft F D & Langenaeker W, *Chem Rev*, 103 (2003) 1793.
39 Parr R G, Szentpaly L & Liu S, *J Am Chem Soc*, 121 (1999) 1922.
40 Chattaraj K & Giri S, *J Phys Chem A*, 111 (2007) 11116.